Evidence for d-wave superconductivity in YBa$_2$Cu$_3$O$_{7-\delta}$ from far-infrared conductivity

J. P. Carbotte, C. Jiang, D. N. Basov, and T. Timusk

Department of Physics and Astronomy, McMaster University, Hamilton, Ontario, Canada L8S 4M1

(Received 1 July 1994; revised manuscript received 28 November 1994)

Calculations of the far-infrared conductivity, which include inelastic as well as arbitrary amounts of elastic impurity scattering, are presented for a superconductor with nodes in the gap. The results are compared with the normal-state conductivity and with previous results for isotropic s-wave superconductors in the clean limit. The effect of adding impurity scattering is also considered, and differences and similarities between the response for s- and d-wave superconductors are noted. The results are compared with recent experimental data on a high-quality single crystal before and after radiation damage. The data are found to be inconsistent with isotropic s waves but display all the expected qualitative features for d waves.

I. INTRODUCTION

Single-crystal YBa$_2$Cu$_3$O$_{7-\delta}$ (YBCO) samples show a large inelastic scattering rate estimated to be of order T_c at temperature $T = T_c$.[1] This illustrates the importance of inelastic scattering at this temperature and clearly indicates the need to include such effects in any complete theory of the infrared response of these superconductors. Another important feature of the high-T_c oxides, which is not in dispute and, indeed, is widely accepted, is the fact that at low temperature they are in the clean limit[1] because of their very short coherence length. To treat these systems then, it is necessary to use a theory of electromagnetic response which includes inelastic as well as arbitrary amounts of elastic (impurity) scattering.[2−5] This situation is in sharp contrast with conventional superconductors where the dirty limit applies. Further, the symmetry of the gap parameter in the superconducting state remains controversial in the oxides with s or d wave being often discussed possibilities,[6−28] while in conventional system it is generally accepted to be s wave.

In a previous paper, Akis, Carbotte, and Timusk[2] have already considered the conductivity in the s-wave case so that here we will start with a formulation which is specifically written for a gap with variation of the form $\Delta = \Delta_0 \cos\theta$ with θ some angle on the Fermi surface ranging from $-\pi$ or π. This form of the gap exhibits zeros and is both positive and negative with equal weight. It is not, strictly speaking, a d-wave gap but will be referred to as d wave in what follows since it has all of the same important physics. The critical feature is that zeros are present and not whether the gap is extended s or d, a point we wish to emphasize here. Section II deals with formalism, Sec. III with results and their discussion, Sec. IV is a comparison with experiment, and conclusions are drawn in Sec. V.

II. FORMALISM

In Nambu notation, the conductivity at frequency v, which is denoted by $\sigma(v)$, can be written in terms of the 2×2 matrix Green's function $G_s(\underline{p}, \omega)$ in the superconducting state with $\underline{p}$ momentum and ω energy. The expression for $\sigma(v)$ is

$$\sigma(v) = \frac{i}{v} \frac{2e^2 v_F^2 N(0)}{3} \left\langle \mathrm{tr} \left\{ \int d\epsilon_{\underline{p}} \int d\Omega \, f(\Omega) \left[-\frac{1}{\pi} \right] \mathrm{Im} G_s(\underline{p}, \Omega + i0^+) \right. \right.$$

$$\left. \left. \times [G_s(\underline{p}, \Omega + v + i0^+) + G_s(\underline{p}, \Omega - v - i0^+)] \right\} \right\rangle , \tag{1}$$

where tr denotes the trace and the brackets $\langle \ \rangle$ indicate an average over the angles θ. The Fermi velocity is v_F, e is the charge on the electron, $N(0)$ is the electronic density of state taken out of the energy integral and pinned to its value at the Fermi surface and $f(\Omega)$ is the Fermi Dirac thermal distribution. The integration over energy $\epsilon_{\underline{p}}$ in Eq. (1) can be carried out and, after considerable algebra, we arrive at a formula for $\sigma(v)$ of the form

$$\sigma(v) = \frac{i}{v} \frac{e^2 N(0) v_F^2}{3} \left\langle \int_0^\infty d\Omega \tanh\left[\frac{\Omega}{2T}\right] \frac{1}{E(\Omega) + E(\Omega+v)} [1 - N(\Omega)N(\Omega+v) - P(\Omega)P(\Omega+v)] \right.$$

$$+ \int_0^\infty d\Omega \tanh\left[\frac{\Omega+v}{2T}\right] \frac{1}{E^*(\Omega) + E^*(\Omega+v)} [1 - N^*(\Omega)N^*(\Omega+v) - P^*(\Omega)P^*(\Omega+v)]$$

$$\times \int_0^\infty d\Omega \left[\tanh\left[\frac{\Omega+v}{2T}\right] - \tanh\left[\frac{\Omega}{2T}\right]\right] \frac{1}{E(\Omega+v) - E^*(\Omega)}$$

$$\times [1 + N^*(\Omega)N(\Omega+v) + P^*(\Omega)P(\Omega+v)] + \int_{-v}^0 d\Omega \tanh\left[\frac{\Omega+v}{2T}\right]$$

$$\times \left[\frac{1}{E^*(\Omega) + E^*(\Omega+v)} [1 - N^*(\Omega)N^*(\Omega+v) - P^*(\Omega)P^*(\Omega+v)]\right.$$

$$\left.\left. + \frac{1}{E(\Omega+v) - E^*(\Omega)} [1 + N^*(\Omega)N(\Omega+v) + P^*(\Omega)P(\Omega+v)]\right]\right\rangle \tag{2}$$

with

$$E(\omega) = \sqrt{\tilde{\omega}_p^2(\omega) - \tilde{\Delta}_p^2(\omega)} \tag{3}$$

and

$$N(\omega) = \frac{\tilde{\omega}_p(\omega)}{E(\omega)}, \quad P(\omega) = \frac{\tilde{\Delta}_p(\omega)}{E(\omega)}, \tag{4}$$

where $\tilde{\Delta}_p(\omega)$ and $\tilde{\omega}_p(\omega)$ are the pairing energy and renormalized Matsubara frequencies, respectively, taken on the real frequency axis and written for the anisotropic state. They are given by Carbotte and Jiang[29] and will not be repeated here. They are the solution of two coupled nonlinear Eliashberg type[29-31] equations appropriate to a model with d-wave pairing which leads to a gap function $\Delta(\theta,\omega)$ of the form $\Delta(\omega)\cos\theta$. The electron-boson spectral density, which we will denote by $\alpha^2 F(\omega)$, is the only parameter that enters in the Eliashberg equations.[29-31] In some models of d-wave pairing, this spectral density would be identified with the antiferromagnetic spin fluctuation[5-28] and the theory of such fluctuations could be used to get some guidance as to its form. Here we will not do this, but simply take it to be some phenomenological form which is then responsible for the pairing in the gap channel as well as for the inelastic scattering of electrons off the relevant bosons of the theory. In addition to the inelastic scattering, impurity scattering in Born approximation can be included in the usual way and described by an elastic-scattering rate πt^+ with $2\pi t^+ \equiv 1/\tau$ with τ the elastic-scattering time. We stress here that specification of this scattering rate and of the electron-boson spectral density completely defines the conductivity provided $\sigma(v)$ here taken in units such that the multiplicative factor $\frac{1}{3}N(0)v_F^2 e^2$ in Eq. (2) is left out and remains unspecified.

In our numerical work, we will use two different choices for the electron-boson spectral density, namely a cutoff Lorentzian introduced by Bickers et al.[4] and later employed in the isotopic s-wave calculations of Akis, Carbotte, and Timusk[2] and, as a second model, the Pb spectrum obtained from tunneling inversion[30] which has weight all the way down to zero frequencies and exhibits a two peak structure at higher energies. Of course, these choices are only for convenience and for definiteness and do not, in any way, commit ourselves to any particular mechanism such as phonons or spin fluctuations, but rather refer simply to some boson exchange mechanism with Migdal-Eliashberg[29-31] equations used as a first approximation in the description of the resulting superconducting state.

III. NUMERICAL RESULTS AND DISCUSSION

In Fig. 1, we show results for the real part of the conductivity (absorptive part) as a function of normalized frequency $\omega/2T_{c0}$ in the far-infrared region of the spectrum. For electron-boson spectral density, a Pb shape[30] was employed and scaled to get a strong-coupling index $T_c/\omega_{\log_{10}} = 0.1$ where $\omega_{\log_{10}}$ is the characteristic boson energy (as defined by Allen and Dynes)[32] associated with the assumed pairing potential. The upper frame applies to the normal state, while the lower frame is for a superconducting state with gap of the form $\Delta(\omega,\theta) = \Delta(\omega)\cos\theta$. The temperatures considered in the figure are solid $T/T_{c0} = 0.985$ long dashed curve $T/T_{c0} = 0.9$, short dashed curve $T/T_{c0} = 0.75$, dotted curve $T/T_{c0} = 0.5$, and solid curve $T/T_{c0} = 0.1$ which is the lowest temperature used in this work. Here T_{c0} is the pure single-crystal critical temperature and the figures apply in the clean limit, i.e., for t^+ set equal to zero. All the curves shown scale with T_{c0} which can therefore be taken to have any desired value. Starting first with the normal-state results (upper frame), we note the Drude peak at low frequencies centered around $\omega = 0$ which is due to scattering of the electrons off the thermally excited bosons. Such bosons act like ordinary impurity scatterers except that now the scattering rate is strongly temperature-dependent and goes to zero at $T = 0$. As a function of frequency, the Drude peak drops rapidly down towards zero as ω is increased and is followed by a region of near zero conductivity before the onset of the
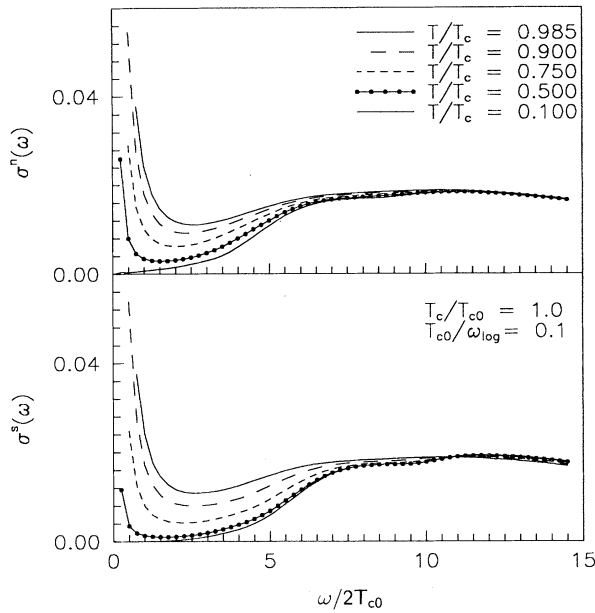
FIG. 1. The real part of the conductivity (in arbitrary units) as a function of normalized frequency $\omega/2T_{c0}$. The upper frame applies to the normal state while the lower frame is for a d-wave superconductor. Both are for the pure limit, no elastic impurities included. The temperatures are $T/T_c=0.985$ (upper solid), $T/T_c=0.9$ (long dashed), $T/T_c=0.75$ (short dashed), $T/T_c=0.5$ (dotted), and $T/T_c=0.1$ (lower solid).

Holstein absorption region at yet higher energies. In the Holstein region, the absorption proceeds through the creation of an electron-hole pair and of an accompanying boson which takes away the extra momentum as well as some energy. The Holstein processes will, of course, reflect the density of boson states as expressed by the spectral density which in our model starts at zero energy with two peaks at roughly $\omega/2T_{c0}=10$ and 20, respectively. Note that, for the solid curve which applies to low temperature namely $T/T_{c0}=0.1$, the Drude peak can no longer be seen any more in our figure and that the Holstein region, which starts at $\omega=0$, sets in gradually and becomes a significant fraction of its value at large frequencies ($\omega/2T_{c0}\cong20$), only at frequencies near the first peak in the spectral density at $\omega/2T_{c0}\cong10$.

We turn now to the superconducting state results shown in the lower frame of Fig. 1. These results were generated with the same parameters as were used in the upper frame but now there is a gap $\Delta(\omega,\theta)$ of the form $\Delta(\omega)\cos\theta$. On comparison with the normal-state results, we note the same general behavior but with two important differences. First, in the superconducting state calculations, the Drude-like contribution is reduced more rapidly with decreasing temperature than it is in the normal state. This is not unexpected since in the superconducting state the normal electron fluid density is reduced with decreasing temperature because of the increased condensation of electrons into Cooper pairs. We note in passing, however, that this effect would not be easy to detect if normal-state curves were not available for com-

parison. Unfortunately, they are not accessible experimentally for the high-T_c oxides. Secondly, the phonon structure in the Holstein region appears shifted to higher energies due to the appearance of a gap. Absorption due to the creation of an electron-hole pair out of the condensate with attendant creation of a boson to take away the extra momentum now proceeds at an energy of twice the gap value plus the lowest boson energy available. While it is true that in a d-wave model the gap can be zero at some points on the Fermi surface and so, strictly speaking, the Holstein processes will start at $\omega=0$ as in the normal state, weight will nevertheless be shifted to higher energies because of the existence of a finite gap at other points on the Fermi surface. This shift is clearly seen in the figure. For an s-wave superconductor with finite isotropic gap value everywhere, the upward shift in boson structure in the superconducting state would, of course, be more pronounced than for the d-wave case indicated in the lower frame of Fig. 1. The s-wave case is shown in Fig. 2 which is reproduced from the previous isotropic s-wave work of Akis, Carbotte, and Timusk[2]. The top frame, which is to one of immediate interest here, applies to the clean limit and was calculated for a spectral density consisting of a cutoff Lorentzian peaked about 50 meV of width 15 meV and with lower cutoff at 15 meV. Its
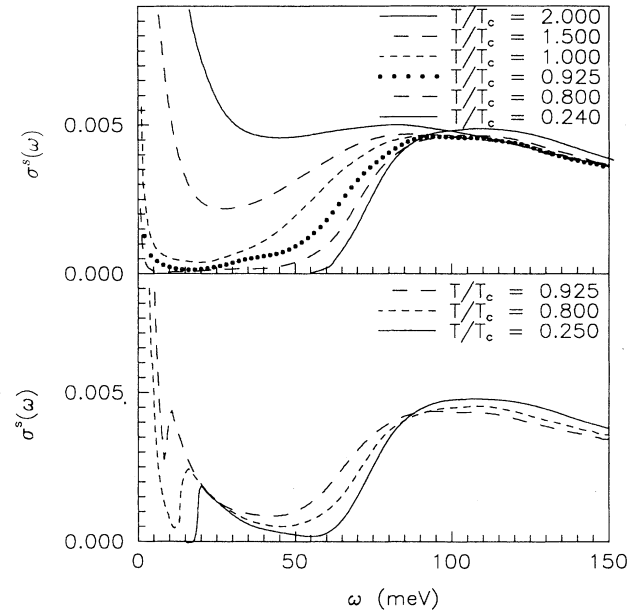

FIG. 2. The real part of the conductivity as a function of frequency ω in meV for a 50 K s-wave superconductor with cutoff Lorentzian spectral density. For the model $\omega_{\log_{10}}=49.3$ meV, $2\Delta_0=17.1$ meV, and $2\Delta_0/k_B T_c=3.97$, moderate coupling. The curves in the upper frame are all in the pure limit, no elastic scattering and apply at different temperature, namely $T=2T_c$ (upper solid line), $T=1.5T_c$ (upper long dashed), and $T=1.0T_c$ (short dashed), $T=0.925T_c$ (dotted), $T=0.8T_c$ (lower long dashed), and $T=0.24T_c$ (lower solid). The curves in the lower frame include some impurity scattering with $t^+=0.17$ meV and are for temperature, $T=0.925T_c$ (long dashed), $T=0.8T_c$ (short dashed), and $T=0.25T_c$ (solid).

strength was adjusted to get a T_{c0} of 50 K. The *s*-wave isotropic gap is $2\Delta_0 = 17.1$ meV and $2\Delta_0/k_B T_c = 3.97$, an intermediate-coupling case. The various curves give the conductivity as a function of frequency for different temperatures. The lowest solid line in the top frame is for $T = 12.5$ K $= 0.25 T_{c0}$ (low temperatures), the long dashed for $T = 40.0$ K $= 0.8 T_{c0}$, dotted for $T = 46.25$ near T_{c0}, short dashed for $T = 50.0$ K $= T_{c0}$, next long dashed for $T = 75.0$ K in the normal state and the upper solid for $T = 100.0$ K. In the solid curve, there is a gap which extends up to $2\Delta_0 = 17.1$ meV plus the lowest boson energy, which is 15 meV, at which point the conductivity rises slowly and quite gradually and becomes large at an energy of $2\Delta_0$ plus the energy of the peak in $\alpha^2 F(\omega)$, which falls at 50 meV. A very important qualitative point to be noted when *s*- and *d*-wave results are compared is that, in the first case, the conductivity in the gap region drops very much more rapidly towards zero with decreasing temperature [compare the lower frame of Fig. 2 (*s*-wave) with the lower frame of Fig. 1 (*d*-wave)]. In fact, this rapid drop in the *s*-wave case and lack thereof in the *d*-wave case can be taken as a qualitative difference between the two cases which could be used when looking at actual conductivity data with an eye at determining the gap symmetry. The present optical data on high-quality single crystals of $YBa_2Cu_3O_{6.95}$ (Refs. 33–37) do not favor *s* wave in this regard as we will discuss more fully later. Also, no region of zero conductivity corresponding to the opening up of a finite gap is ever observed at low temperatures. (See the lower darker solid curve in the lower frame of Fig. 5.) It should be mentioned, however, that the data are also not in accord with our clean limit *d*-wave results given in Fig. 1. The more rapid reduction, in the low-frequency region, of the conductivity noted for an *s*-wave as compared with a *d*-wave superconductor is due mainly to the very different properties of the condensate in the two cases and has little to do with a racial difference in scattering rate. First of all, it is only the normal electrons that can be usefully described in terms of classical ideas such as associated scattering rate. Such ideas do not apply to the electrons in the superfluid fraction which will not absorb energy unless the photon energy is twice the gap value and so make no contribution to the conductivity for such frequencies. But in contrast to an *s*-wave superconductor, in the *d*-wave case, some electrons at the Fermi surface have zero or near zero gap and direct absorption through pair breaking is always possible. Also, the normal fluid increases more rapidly with temperature. Both effects give more low-frequency absorption relative to the *s*-wave case. The shape of the conductivity curves in this region has little to do with differences in normal fluid scattering rate which, in any case, cannot be measured directly in optical experiments as one cannot separate normal and pair-breaking parts.

An important conclusion that can be made from the discussion so far is that, in the pure case including only inelastic scattering, it is difficult to identify a value for the gap and distinguish clearly a *d*-wave superconductor from a normal metal as the curves will look qualitatively similar, although more definitive conclusions, could be reached if normal-state data were also available for com-

parison with the superconductor-state data. Unfortunately, in the high-T_c oxides, the low-temperature normal state is not accessible to us, and only the superconducting-state curves are known.

Next, we account for some normal elastic scattering through a finite value of the impurity scattering rate t^+. We will see that an isotropic *s*-wave superconductor will react quite differently to the introduction of t^+ than will a *d*-wave superconductor. A first difference is that t^+ does not affect the size of the critical temperature T_{c0} in an isotropic *s*-wave superconductor because of Anderson's theorem,[38] while in the *d*-wave case, T_c is reduced from its pure crystal value T_{c0} because of the washing out of anisotropy by the elastic scattering. The optical response is also very different in these two cases. An obvious first effect on the conductivity of the introduction of a finite t^+ is that the low-frequency Drude peak should broaden and its width related to the sum of elastic- plus inelastic-scattering rates. Second, a new impurity-assisted absorption channel will open. It now becomes possible to create a hole particle pair out of the condensate without attendant boson to conserve momentum. This new process will have a sharp onset at $2\Delta_0$ in an *s*-wave superconductor and be peaked about this energy as is shown in the lower frame of Fig. 2 which is again reproduced from the earlier work of Akis, Carbotte, and Timusk.[2] In these curves, the elastic-scattering rate has been set at $t^+ = 0.17$ meV. The curves apply to the conductivity in the superconducting state and are for three different temperature, namely the solid curve $T = 12.5$ K $= 0.25 T_{c0}$ (low temperature), short dashed curve for $T = 40.0$ K $= 0.8 T_{c0}$ and long dashed curve for $T = 46.25$ K (near T_{c0}). In the low-temperature curve, the conductivity is zero up to $2\Delta_0 = 17.1$ meV and then shows an abrupt absorption edge which peaks at $2\Delta_0$. This feature can, in principle, be used to measure the zero-temperature gap value. As well, the temperature dependence of the gap can be tracked through the same gap feature which persists at higher temperature although now it is superimposed on a sharply increasing Drude background. There is no trace of any of these features in the experimental data shown in the lower frame of Fig. 5 for $YBa_2Cu_3O_{6.95}$ which we will discuss later.

The effect of impurity scattering is quite different in the *d*-wave case. This is shown in Figs. 3 and 4. Figure 3 applies to a case in which T_c has been reduced by 5% by the impurities, while in Fig. 4, a 20% reduction in T_c is involved, i.e., $T_c/T_{c0} = 0.8$. In each of the two figures, the top frame gives the normal-state conductivity and the bottom frame, the superconducting state. The temperatures are $T/T_c = 0.1$ (lower solid curve), $T/T_c = 0.5$ (dotted curve), $T/T_c = 0.75$ (short dashed curve), $T/T_c = 0.9$ (long dashed curve), and $T/T_c = 0.985$ (upper solid curve). It is clear from the figures that, in each case, the elastic scattering is of the same order of magnitude as the inelastic scattering although the remaining temperature variation of the normal-state conductivity is already quite small in Fig. 4. Further, while a minimum still occurs around $\omega/2T_{c0} \cong 5$, it is not as deep as in the clean limit, and the conductivity in this region is reduced over its
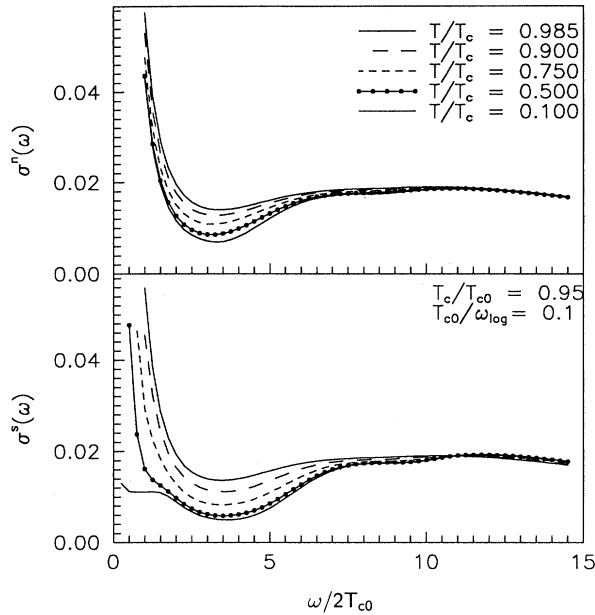
FIG. 3. The real part of the conductivity (in arbitrary units) as a function of normalized frequency $\omega/2T_{c0}$. The upper frame applies to the normal state, while the lower frame is for a d-wave superconductor. Impurity scattering is included in Born approximation with t^+ large enough to reduce the critical temperature by 5%. The temperatures are as in Fig. 1.
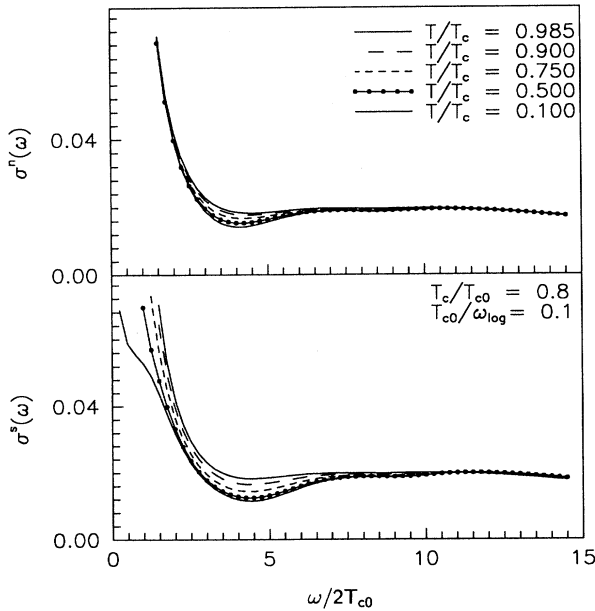

FIG. 4. Same as Fig. 3 but now the critical temperature has been reduced to 80% of its pure value through impurity scattering.

large frequency limit by approximately a factor of 2. Comparing our normal-state results with the corresponding superconducting state results, we note that the superconducting state conductivity in Fig. 3 shows a much greater temperature dependence than its normal-state counterpart and that the value of conductivity is also generally reduced as might have been expected since the density of electronic states is depressed in the gap region even for a d-wave superconductor. The solid curve at low temperature is the most important and is in striking contrast to the s-wave case (lower frame of Fig. 2). The conductivity now remains quite finite at all the optical frequencies shown and has a nearly constant region centered around $\omega/2T_{c0} \cong 2.5$ which is the frequency of the peak in the corresponding quasiparticle density of states. The flat region extends over an energy range of $\omega/2T_{c0} \cong 2$ and is followed by a sharp upturn in conductivity at lower energies. The knee at $\omega/2T_{c0} = 3.5$ and the flat region develop into a shoulder in the lower frame of Fig. 4 which applies to a higher impurity scattering rate than in Fig. 3. It corresponds to a 20% reduction in the pure crystal critical temperature T_{c0}. The position of the center of the shoulder is at roughly $\omega/2T_{c0} = 2.0$ which is the position of the peak in the quasiparticle density of states in this case. While we will make no attempt whatsoever to fit the available experimental data to our calculations, we want to point out that the results of Figs. 3 and 4 have all of the qualitative features observed experimentally.

IV. COMPARISON WITH EXPERIMENT

In Fig. 5, we compare the results of our calculations with the experimental data for the ab-plane conductivity of YBa$_2$Cu$_3$O$_{6.95}$ single crystal measured by Basov et al.[33] The experimental conductivity is shown in the bottom panel for $T = 10$ K for the nonirradiated crystal and for the same sample after it has been irradiated with low-energy He ions so that T_c has been suppressed from 93.5 down to 80 K. The upper panel presents the calculated conductivity at $T = 0.1T_c$ for different amounts of impurities. It is important to realize that the present data in the high-quality nonirradiated crystal exhibit a finite conductivity at all frequencies and does not look qualitatively like the pattern predicted for the clean limit in the s wave (Fig. 2) and even in the d wave (Fig. 1). We note, though, the similarities between the experimental curve for the nonirradiated sample and the theoretical curve for the lowest level of impurity when $T_c = 0.985T_{c0}$ (Fig. 3). The predicted flat region at low frequencies ($\omega < 150$ cm^{-1}) is nicely reproduced in the experimental data. Also, the value of the conductivity in the dip region around 500 cm^{-1} is roughly a factor of 2 lower than its high-frequency value (at about 1000 cm^{-1}). These data, which were taken on the best crystal available, would seem to indicate that some intrinsic Born scattering remains in these crystals and would need to be sufficient to account for about a 5% percent reduction in T_c value as in our Fig. 3.

The striking property of the irradiated crystal is a narrow Drude-like feature at low frequencies whereas the

light-frequency behavior does not seem to be affected as much by ion damage. We believe that this narrow component is present in the conductivity of the nonirradiated sample as well, consistent with microwave results on the crystals from the same batch,[39] but remains unachievable for a far-infrared probe because of the small value of the scattering rate. Irradiation not only increases the width of this component of the conductivity but also enhances it spectral weight.[33]

Similar effect has been observed in the conductivity of the single crystal with inclusion of 5% of Ni.[40] This property of lightly disordered YBCO samples is reproduced by the calculations for the next amount of scattering when T_c is further suppressed down to $0.8 \times T_{c0}$. We also note the shoulder in the data around 200 cm^{-1} is present in the calculated spectrum as well. In addition, the dip in the conductivity close to 500 cm^{-1} is getting weaker both in the experimental and the theoretical curves. While the agreement with the calculations shown by Fig. 5 is certainly not quantitative, much qualitative agreement is nevertheless seen. In this regard, we note that we have in no way tried to adjust the amount of inelastic scattering present in our theory so as to get a best fit to the data. Our calculations are mainly illustrative.
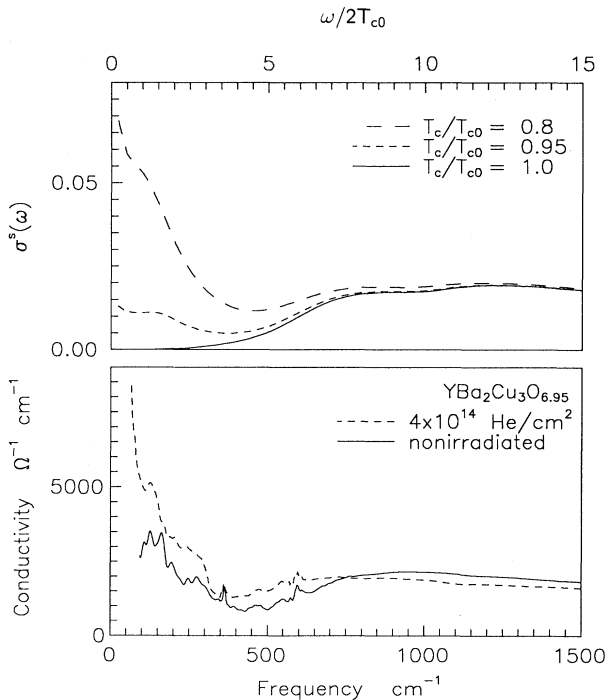

FIG. 5. Top panel: calculated conductivity at $T = 0.1T_c$ for clean d-wave superconductor (solid line) and for the d-wave superconductor with two different amounts of impurities when T_c is suppressed down to $0.95T_{c0}$ (short dashed line) and down to $0.8T_{c0}$ (long dashed line). Bottom panel: experimental ab-plane conductivity of a $YBa_2Cu_3O_{6.95}$ single crystal from Ref. 33. Solid line is the conductivity of nonirradiated crystal with $T_c = 93.5$ K, dashed line is the conductivity of the same crystal irradiated with 4×10^{14} He/cm^2 in which case T_c is suppressed down to 80 K.

By contrast, the s-wave response in the superconducting state (Fig. 2) does not agree with any of the experimental features shown in Fig. 5. With impurities added to the s-wave superconductor the conductivity shows a sharp edge and peak at twice the isotropic energy gap value. This feature, which is predicted to be quite prominent, is never seen in the experimental data even in dirty samples.[33,41,42,40] It is, however, not expected for a d-wave case for which the gap has zeros on the Fermi surface. Impurities have different effects on the conductivity spectra in the s-wave and d-wave scenarios: in the s-wave case impurities induce a gap structure at 2Δ whereas in the d-wave case the defects generate a Drude-like absorption extending all the way to zero frequency.

As suggested above, even in the high-quality single crystal used for the far-infrared experiments of Ref. 33, a small amount of weak elastic scattering is present and needs to be sufficient to reduce the sample critical temperature of the sample by about 5% as compared to a hypothetical disorder-free sample. The existence of Born scattering at this level is in no way inconsistent with the linear dependence of the penetration depth found in crystals from the same batch.[7] While resonance scattering, for example by Zn impurities, would lead to a T^2 dependence at the 5% reduction level in T_c,[43] this is not the case for Born scattering which starts to change significantly from the linear law only at much higher concentrations corresponding to 30% reduction of T_c.[19] We emphasize, that even in the irradiated crystal with the critical temperature being equal to 0.885 of the T_c of the nonirradiated sample, a marked deviation from the T^2 law has been found.[33] Only with higher level of ion damage, when the transition temperature is further suppressed down to 0.75 of the initial T_c, the crossover to $T^n (2 < n < 4)$ behavior observed.[33]

Comparison of the experimental results with our theory indicates that characteristic features of the infrared conductivity and their transformation with disorder are in agreement with the d-wave approach. We have not attempted, in any way, to find a best fit of the theory to the data by adjusting the boson region or the impurity scattering. Qualitatively, however, we can understand all observed features and can conclude, quite unambiguously, that the data are inconsistent with the isotropic s-wave, while it displays many of the features expected when the gap has a zero on the Fermi surface.

For the purpose of a quantitative comparison with the theory presented, several other factors have to be taken into consideration. In the frequency region of the Holstein absorption discussed in this paper, other contributions to the conductivity are of importance. First, the in-plane response of the YBCO system is known to be strongly anisotropic along Cu-O chains (b axis) and in the direction perpendicular to the chains (a axis).[44,45,36,46] While the effect of impurities has been not studied directly in the untwinned samples, the comparison of the optical data obtained on the recently available high-quality crystals[46] with data on earlier samples[44,45] suggests that the chains may be extremely sensitive to even a weak disorder. Thus, a quantitative comparison with theory should be performed for the a-axis conductivity of an

untwinned crystal. In addition to this, it has been shown by Reedyk and Timusk that coupling to the c-axis longitudinal phonons may be responsible for dips in the ab-plane far-infrared conductivity.[47] This effect, however, is not important when the in-plane conductivity is obtained from reflectance measurements performed on the lateral surface of a crystal. Finally, we note that the residual scattering that we suggest for the nonirradiated single crystal of $YBa_2Cu_3O_{6.95}$ may be due to the deviation of this compound from stoichiometry. It is then preferable to investigate disorder effects in the stoichiometric $YBa_2Cu_4O_8$ superconductors which in addition is intrinsically untwinned.

V. CONCLUSIONS

We have presented results of calculations for the infrared conductivity of a superconductor with nodes in the energy gap. We have fully included in our theory the inelastic scattering provided by the bosons responsible for the superconducting state which might be the antiferromagnetic spin fluctuations. Elastic scattering from an arbitrary concentration of impurities in Born approximation was also considered. We discussed the qualitative difference between the impact of impurities on the far-infrared conductivity of s-wave and d-wave superconductors.

We compared the results of our calculations with experimental studies of disorder effects in high-quality single crystals of $YBa_2Cu_3O_{6.95}$. We found that the d-wave scenario is consistent with these data whereas there is clear qualitative disagreement between experiment and the theory for the s-wave case. To end, we stress that everything we have found is valid for any gap parameter which exhibits zeros on the Fermi surface and has regions of positive and negative values of the gap and exists for extended s-wave equally well.

ACKNOWLEDGMENTS

[1] T. Timusk and D. B. Tanner, in *Physical Properties of High Temperature Superconductors I*, edited by D. M. Ginsberg (World Scientific, Singapore, 1989), p. 339.

[2] R. Akis, J. P. Carbotte, and T. Timusk, Phys. Rev. B **43**, 12 804 (1991).

[3] W. Lee, D. Rainer, and W. Zimmermann, Physica C **159**, 535 (1989).

[4] N. E. Bickers, D. J. Scalapino, R. T. Collins, and Z. Schlesinger, Phys. Rev. B **42**, 67 (1990).

[5] E. Nicol, J. P. Carbotte, and T. Timusk, Phys. Rev. B **43**, 473 (1991).

[6] Z. K. Shen and D. S. Dessau *et al.*, Phys. Rev. Lett. **70**, 1553 (1993).

[7] W. Hardy *et al.*, Phys. Rev. Lett **70**, 3999 (1993).

[8] J. F. Annett and N. Goldenfeld, J. Low Temp. Phys. **89**, 197 (1992).

[9] N. E. Bickers, R. T. Scalettar, and D. J. Scalapino, Int. J. Mod. Phys. B **1**, 687 (1987).

[10] S. Wermbter and L. Tewordt, Phys. Rev. B **43**, 10 530 (1991).

[11] H. Monien, P. Monthoux, and D. Pines, Phys. Rev. B **43**, 275 (1991).

[12] M. R. Norman, Phys. Rev. B **37**, 4987 (1988); **41**, 170 (1990).

[13] D. Pines, Physica C **185-189**, 120 (1991).

[14] R. J. Radtke, S. Ullah, K. Levin, and M. R. Norman, Phys. Rev. B **46**, 11 975 (1992).

[15] E. J. Nicol, C. Jiang, and J. P Carbotte, Phys. Rev. B **47**, 8131 (1993).

[16] P. Monthoux and D. Pines, Phys. Rev. Lett **69**, 961 (1992).

[17] N. Bulut and D. J. Scalapino, Phys. Rev. B **45**, 2371 (1992).

[18] St. Lenck and J. P. Carbotte, Phys. Rev. B **46**, 14 850 (1992).

[19] P. Arberg, M. Mansor, and J. P. Carbotte, Solid State Commun. **86**, 671 (1993).

[20] P. Monthoux and D. Pines, Phys. Rev. B **47**, 6069 (1993).

[21] Y. Zha, K. Levin, and Qimiao Si, Phys. Rev. B **47**, 9124 (1993).

[22] Q. Si, Y. Zha, K. Levin, and J. P. Lu, Phys. Rev. B **47**, 9055 (1993).

[23] C. Jiang, J. P. Carbotte, and R. C. Dynes, Phys. Rev. B **47**, 5325 (1993).

[24] A. Perez-Gonzalez and J. P. Carbotte, Phys. Rev. B **45**, 9894 (1992).

[25] C. T. Rieck, D. Fay, and L. Tewordt, Phys. Rev. B **41**, 7289 (1990).

[26] L. Tewordt and Th. Wölkhausen, Solid State Commun. **75**, 515 (1990).

[27] L. Tewordt, S. Wermbter, and Th. Wölkhausen, Phys. Rev. B **40**, 6878 (1989).

[28] L. Tewordt, D. Fay, and Th. Wölkhausen, Solid State Commun. **67**, 301 (1988).

[29] J. P. Carbotte and C. Jiang, Phys. Rev. B **48**, 4231 (1993).

[30] J. P. Carbotte, Rev. Mod. Phys. **62**, 1027 (1990).

[31] F. Marsiglio, M. Schossmann, and J. P. Carbotte, Phys. Rev. B **37**, 4965 (1988).

[32] P. B. Allen and R. C. Dynes, Phys. Rev. B **12**, 905 (1975).

[33] D. N. Basov, A. V. Puchkov, R. A. Hughes, T. Strach, J. Preston, T. Timusk, D. A. Bonn, R. Liang, and W. N. Hardy, Phys. Rev. B **49**, 12 165 (1994).

[34] D. B. Tanner and T. Timusk, in *Physical Properties of High Temperature Superconductors III*, edited by D. M. Ginsberg (World Scientific, Singapore, 1992).

[35] K. F. Renk, B. Gorshunov, J. Shutzmann, A. Prückl, B. Brunner, J. Betz, S. Orbach, N. Klein, G. Müller, and H. Piel, Europhys. Lett. **15**, 661 (1991).

[36] T. Pham, M. W. Lee, H. D. Drew, U. Welp, and Y. Fang, Phys. Rev. B **44**, 5377 (1991).

[37] D. M. Miller, P. L. Richards, S. Estmad, A. Inam, T. Venkatesan, B. Dutta, X. D. Wu, C. B. Eom, T. H. Geballe, N. Newman, and B. B. Cole, Phys. Rev. B **47**, 8076 (1993).

[38] P. W. Anderson, J. Phys. Chem. Solids **11**, 26 (1959).

[39] D. A. Bonn and R. Liang *et al.*, Phys. Rev. B **47**, 11 314

(1993).

[40]C. C. Homes, Q. Song, B. P. Clayman, R. Liang, D. A. Bonn, and W. N. Hardy (unpublished).

[41]D. Mandrus, M. C. Martin, C. Kendziora, D. Keller, L. Forro, and L. Mihaly, Phys. Rev. Lett. **70**, 2629 (1993).

[42]M. J. Sumner, J.-T. Kim, and T. R. Lemberger, Phys. Rev. B **47**, 12 248 (1993).

[43]D. Achkir, M. Poirier, D. A. Bonn, R. Liang, and W. N. Hardy, Phys. Rev. B **48**, 13 184 (1993).

[44]Z. Schlesinger, R. T. Collins, F. Holtzberg, C. Field, S. H. Blanton, U. Welp, G. W. Crabtree, Y. Fang, and J. Z. Liu, Phys. Rev. Lett. **65**, 801 (1990).

[45]Z. Schützmann, B. Gorshunov, K. F. Renk, J. Münzel, A. Zibold, H. P. Geserich, A. Erb, and G. Müller-Vogt, Phys. Rev. B **46**, 512 (1992).

[46]D. N. Basov, R. Liang, D. A. Bonn, W. N. Hardy, B. Dabrowksi, M. Quijada, D. B. Tanner, J. P. Rice, D. M. Ginsberg, and T. Timusk, Phys. Rev. Lett. **74**, 598 (1995).

[47]M. Reedyk and T. Timusk, Phys. Rev. Lett. **69**, 2705 (1992).